



**Analytical approach
for determining mean
water level profile**

H. Cai et al.

This discussion paper is/has been under review for the journal Hydrology and Earth System Sciences (HESS). Please refer to the corresponding final paper in HESS if available.

Analytical approach for determining the mean water level profile in an estuary with substantial fresh water discharge

H. Cai¹, H. H. G. Savenije², C. Jiang³, L. Zhao⁴, and Q. Yang¹

¹Institute of Estuarine and Coastal Research, School of Marine Science, Sun Yat-sen University, Guangzhou 510275, China

²Water Resources Section, Delft University of Technology, Delft, the Netherlands

³School of Hydraulic, Energy and Power Engineering, Yangzhou University, Yangzhou 225127, China

⁴State Key Laboratory of Hydrology and Hydraulic Engineering, Hohai University, Nanjing 210098, China

Received: 7 August 2015 – Accepted: 12 August 2015 – Published: 26 August 2015

Correspondence to: Q. Yang (yangqsh@mail.sysu.edu.cn)

Published by Copernicus Publications on behalf of the European Geosciences Union.

Title Page

Abstract

Introduction

Conclusions

References

Tables

Figures



Back

Close

Full Screen / Esc

Printer-friendly Version

Interactive Discussion



Abstract

Although modestly, the mean water level in estuaries rises in landward direction induced by a combination of the salinity gradient, the tidal asymmetry, and the backwater effect. The water level slope is increased by the fresh water discharge. However, the interactions between tide and river flow and their individual contributions to the rise of the mean water level along the estuary are not yet completely understood. In this study, we adopt an analytical approach to describe the tidal wave propagation under the influence of fresh water discharge, in which the friction term is approximated by a Chebyshev polynomials approach. The analytical model is used to quantify the contributions made by tide, river, and tide–river interaction to the water level slope along the estuary. Subsequently, the method is applied to the Yangtze estuary under a wide range of river discharge conditions and the influence of tidal amplitude and fresh water discharge on the longitudinal variation of mean water level is explored. The proposed method is particularly useful for accurately predicting water levels and the frequency of extreme high water, relevant for water management and flood control.

1 Introduction

It is of both theoretical and practical importance to understand the dynamics of wave propagation under backwater effect, for instance when a river is backed up by an obstruction, such as a weir or a bridge, by a confluence with a larger river, or by an ocean tide, resulting in a rise of the water level upstream of the obstruction. Generally, the backwater effect can be quantified by using the variation of the water level slope in the momentum equation. Many researchers have explored the backwater effect in open channels by disregarding one or more terms in the momentum equation (detailed review can be found in Dottori et al., 2009). Among them, the most well-known is Jones' formula (Jones, 1916), which is an analytical expression of the water level slope as a function of fresh water discharge and geometric characteristics (e.g., bottom slope,

HESSD

12, 8381–8417, 2015

Analytical approach for determining mean water level profile

H. Cai et al.

Title Page

Abstract

Introduction

Conclusions

References

Tables

Figures

◀

▶

◀

▶

Back

Close

Full Screen / Esc

Printer-friendly Version

Interactive Discussion



cross-sectional area, hydraulic radius, Manning's coefficient). However, the backwater effect induced by an ocean tide in interaction with a river flood in an estuary still remains subject for further investigation.

It has been suggested that the mean water surface of a tidal river is driven by the fortnightly fluctuation due to the spring-neap changes in tidal amplitude at the seaward side, but it also features a consistent increase in landward direction, caused by the tide–river interaction (e.g., LeBlond, 1979; Godin and Martinez, 1994; Buschman et al., 2009; Sassi and Hoitink, 2013) and the density gradient (e.g., Savenije, 2005, 2012). The key to understand the interplay between tide and fresh water discharge in an estuary lies in the friction term of the momentum equation, which is usually decomposed into different components contributed by tide, river and tide–river interaction (Dronkers, 1964; Godin, 1991, 1999; Buschman et al., 2009; Sassi and Hoitink, 2013). In particular, Dronkers (1964) used the Chebyshev polynomials approach to approximate the quadratic velocity in the friction term, in which the resulted approximation consists of four terms with coefficients depending on the ratio between river flow velocity and tidal velocity amplitude. Godin (1991, 1999) proposed a simpler approximation that retains only the first and third order terms as a function of the nondimensionalized velocity, which is comparable with Dronkers' formula in terms of accuracy.

It was shown by Godin (1999) that the sub-tidal water level can be reconstructed by a simple linear regression equation as a function of fresh water discharge and tidal range, suggesting a strong correlation between sub-tidal water level and tide–river interaction. To understand the basic mechanisms of the tide–river interaction in the Columbia river, Jay and Flinchem (1997) and Kukulka and Jay (2003a, b) employed a wavelet tidal analysis method to decompose the time series of water levels into different components (diurnal, semi-diurnal, quarter-diurnal and mean flow), which allows taking account of the tidal asymmetry (i.e., interaction between different tidal constituents). They also derived a linear regression model for describing the sub-tidal water level as a function of fresh water discharge, tidal range, and atmospheric pressure. Similar linear regression models were proposed by Buschman et al. (2009); Sassi

HESSD

12, 8381–8417, 2015

Analytical approach for determining mean water level profile

H. Cai et al.

[Title Page](#)

[Abstract](#)

[Introduction](#)

[Conclusions](#)

[References](#)

[Tables](#)

[Figures](#)



[Back](#)

[Close](#)

[Full Screen / Esc](#)

[Printer-friendly Version](#)

[Interactive Discussion](#)



and Hoitink (2013) and Guo et al. (2015) for predicting the sub-tidal water level on the basis of the decomposed sub-tidal friction in the momentum equation. In addition, Jay et al. (2015) demonstrated that power spectra, continuous wavelet transforms, and harmonic analyses are useful instruments to understand external changes (e.g., tide, river flow, upwelling and down-welling) on the variations of along-channel water level. In this contribution, we adopt an analytical model for tidal hydrodynamics (Cai et al., 2014b) to quantify the contributions made by the tidal flow, the river flow and the interaction between tide and river flow to the water level surface gradient in a tidal river. We only focus on the interaction between the predominant tidal constituent (e.g., M_2) and the river flow, aiming to derive fully explicit analytical expressions describing the basic mechanisms that cause the rise of mean water level along the estuary.

The density-induced pressure in the momentum equation is upstream-directed and counteracted by a residual water level that equals to 1.25 % of the mean water depth over the length of salt intrusion, having a significant influence on salt intrusion through gravitational circulation (Savenije, 2005, 2012). In the Yangtze estuary the water level rise due to the density gradient is around 0.12 m (corresponding to an estuary depth of 9.5 m) over the salt intrusion length (approximately 50 km). Thus the density-induced slope is rather small (around 3.0×10^{-8}) compared to the frictional dissipation induced by river discharge. Consequently, we neglect the effect of the density gradient on the mean water level profile in this paper.

In the following section, the general methodology for describing the tidal wave propagation under riverine influence and contributions made by different frictional components (river, tide, tide–river interaction) to the rise of mean water level are presented. This is followed by an application to the Yangtze estuary where there is a notable influence of fresh water discharge on tidal dynamics (Sect. 3). We explored the response of the mean water level as a function of tidal forcing imposed at the mouth and the fresh water discharge from upstream. Subsequently, the method has been used to predict the envelopes of high water and low water in the Yangtze estuary. In particular, it is shown that the analytical model can be used to estimate the likelihood of extreme high

HESSD

12, 8381–8417, 2015

Analytical approach for determining mean water level profile

H. Cai et al.

Title Page

Abstract

Introduction

Conclusions

References

Tables

Figures



Back

Close

Full Screen / Esc

Printer-friendly Version

Interactive Discussion



water levels along the estuary for given probability of exceedence. Finally, conclusions are summarized in Sect. 4.

2 Methodology

2.1 Shape of an estuary

5 For the derivation of analytical solutions of the tidal hydrodynamics equations in estuaries, we require geometric functions to describe the estuary geometry, such as constant geometry (e.g., Ippen, 1966), a linear function (e.g., Gay and O'Donnell, 2007, 2009), a power function (e.g., Prandle and Rahman, 1980) or an exponential function (e.g., Savenije, 1998, 2001, 2005, 2012). Among these, the most common approach is to
10 use an exponential function to describe the cross-sectional area, width and depth in a tidally averaged scale. This method works very well in a tide-dominated estuary, which usually has a typical funnel shape. However, as opposed to what is generally done, the cross-sectional area and stream width do not converge to zero, but to constant river dominated values. To better represent the geometry of such funnel-prismatic
15 estuaries, we propose the following expressions to describe the longitudinal variation of cross-sectional area \bar{A} and stream width \bar{B} (see also Toffolon et al., 2006; Cai et al., 2014b):

$$\bar{A} = \bar{A}_r + (\bar{A}_0 - \bar{A}_r) \exp\left(-\frac{x}{a}\right) \quad (1)$$

$$\bar{B} = \bar{B}_r + (\bar{B}_0 - \bar{B}_r) \exp\left(-\frac{x}{b}\right) \quad (2)$$

20 where x is the distance (starting from the estuary mouth), \bar{A}_0 and \bar{B}_0 represent the cross-sectional area and stream width evaluated at the estuary mouth, \bar{A}_r and \bar{B}_r represent the asymptotic riverine cross-sectional area and stream width, while a and b

Analytical approach for determining mean water level profile

H. Cai et al.

Title Page

Abstract

Introduction

Conclusions

References

Tables

Figures

⏪

⏩

◀

▶

Back

Close

Full Screen / Esc

Printer-friendly Version

Interactive Discussion



represent the convergence lengths of the cross-sectional area and stream width, respectively. This equation not only accounts for the exponential shape in the seaward part of the estuary, but also the nearly prismatic channel in the landward part. Assuming a near rectangular cross-section, the tidally averaged depth is given by $\bar{h} = \bar{A}/\bar{B}$.

Figure 1 illustrates the variation of the estuarine shape for different convergence lengths. In this approach, there is no need for an inflection point to cater for the transition from a funnel shape to a prismatic channel.

2.2 Analytical model for tidal hydrodynamics

In a tidal river, we usually observe that the tidally averaged water level rises in landward direction. This residual water level increases with the fresh water discharge. In order to explore the underlying mechanism of this phenomenon and quantify the contributions of tide, river and tide–river interaction to the increased residual water level, analytical solutions are invaluable tool since it provides direct insight into the tidal wave propagation under the influence of river discharge. It has been suggested by Cai et al. (2014a, b) that the hydrodynamics in a tidal river is mainly determined by the four dimensionless parameters (see Table 1), including the tidal amplitude to depth ratio ζ (representing the boundary condition in the seaward side), the estuary shape number γ (indicating the channel convergence), the friction number χ (representing the frictional dissipation), and the dimensionless river discharge φ (representing the effect of fresh water discharge), where η is the tidal amplitude, v is the velocity amplitude, U_r is the river flow velocity, ω is the tidal frequency, g is the gravity acceleration, K is the Manning–Strickler friction coefficient, r_S is the storage width ratio, and c_0 is the classical wave celerity defined as $c_0 = \sqrt{g\bar{h}/r_S}$. It is important to recognize that we use a new definition for the estuary shape number as suggested by Cai et al. (2014b) to account for the asymptotic adjustment to the river cross-section, the difference being a factor $(1 - \bar{A}_r/\bar{A})$, which varies with distance although it remains close to unity in the most downstream reach of the estuary.

Analytical approach for determining mean water level profile

H. Cai et al.

Title Page

Abstract

Introduction

Conclusions

References

Tables

Figures



Back

Close

Full Screen / Esc

Printer-friendly Version

Interactive Discussion



Analytical approach for determining mean water level profile

H. Cai et al.

Title Page

Abstract

Introduction

Conclusions

References

Tables

Figures

⏪

⏩

◀

▶

Back

Close

Full Screen / Esc

Printer-friendly Version

Interactive Discussion



We use the analytical model for tidal dynamics proposed by Cai et al. (2014a, b), in which the solutions of the main tidal dynamics are obtained by means of solving a set of four implicit equations for the main dynamics, including tidal damping or amplification, wave celerity (or speed), velocity amplitude and phase lag. The main dependent parameters are described by the following four variables (see Table 1): δ represents the amplification number describing the damping ($\delta < 0$) or amplified ($\delta > 0$) rate of along-channel tidal amplitude, μ the velocity number indicating the ratio of actual velocity amplitude to that in a frictionless prismatic channel, λ the celerity number representing the classical wave celerity c_0 scaled by the actual wave celerity (speed) c , and ε representing the phase lag between high water (HW) and high water slack (HWS) or between low water (LW) and low water slack (LWS). It is noted that $0 \leq \varepsilon \leq \pi/2$, where $\varepsilon = 0$ indicates the tidal wave characterized by a standing wave, while $\varepsilon = \pi/2$ suggesting a progressive wave. For a predominant tide (e.g., M_2), the phase lag is determined by $\varepsilon = \pi - (\phi_Z - \phi_U)$, in which ϕ_Z and ϕ_U represent the phase of water level and velocity, respectively (Savenije et al., 2008). The set of four dimensionless equations are given by Cai et al. (2014b):

the tidal damping equation, describing the tidal amplification or damping as a result of the balance between convergence ($\gamma\theta$) and friction ($\chi\mu\lambda\Gamma$):

$$\delta = \frac{\mu^2(\gamma\theta - \chi\mu\lambda\Gamma)}{1 + \mu^2\beta}, \quad (3)$$

the scaling equation, describing how the ratio of velocity amplitude to tidal amplitude depends on phase lag and wave speed (wave celerity):

$$\mu = \frac{\sin(\varepsilon)}{\lambda} = \frac{\cos(\varepsilon)}{\gamma - \delta}, \quad (4)$$

the wave celerity (or speed) equation, describing how the wave speed depends on the balance between convergence and tidal damping/amplification:

$$\lambda^2 = 1 - \delta(\gamma - \delta), \quad (5)$$

the phase lag equation, describing how the phase lag between HW and HWS depends on wave speed, convergence and damping:

$$\tan(\varepsilon) = \frac{\lambda}{\gamma - \delta}, \quad (6)$$

where θ , β and Γ account for the effect of river discharge, and where:

$$\Gamma = \frac{1}{\pi} \left[\rho_1 - 2\rho_2\varphi + \rho_3\varphi^2(3 + \mu^2\lambda^2/\varphi^2) \right], \quad (7)$$

is a friction factor obtained by using Chebyshev polynomials (Dronkers, 1964) to represent the non-linear friction term in the momentum equation:

$$F = \frac{U|U|}{K^2 h^{-4/3}} \approx \frac{1}{K^2 h^{-4/3} \pi} \left(\rho_0 v^2 + \rho_1 vU + \rho_2 U^2 + \rho_3 U^3/v \right), \quad (8)$$

in which U is the cross-sectionally averaged velocity consisting of a steady component U_r , generated by the fresh water discharge, and a time-dependent constituent U_t , introduced by the tidal flow:

$$U = U_t - U_r = v \sin(\omega t) - Q/\bar{A}, \quad (9)$$

where t is time and Q is the fresh water discharge (treated as a constant during the tidal wave propagation), and ρ_i ($i = 0, 1, 2, 3$) represent the Chebyshev coefficients (see Dronkers, 1964, p. 301), which are functions of φ through $\alpha = \arccos(-\varphi)$:

$$\rho_0 = -\frac{7}{120} \sin(2\alpha) + \frac{1}{24} \sin(6\alpha) - \frac{1}{60} \sin(8\alpha), \quad (10)$$

$$\rho_1 = \frac{7}{6} \sin(\alpha) - \frac{7}{30} \sin(3\alpha) - \frac{7}{30} \sin(5\alpha) + \frac{1}{10} \sin(7\alpha), \quad (11)$$

$$\rho_2 = \pi - 2\alpha + \frac{1}{3} \sin(2\alpha) + \frac{19}{30} \sin(4\alpha) - \frac{1}{5} \sin(6\alpha), \quad (12)$$

Analytical approach for determining mean water level profile

H. Cai et al.

Title Page

Abstract

Introduction

Conclusions

References

Tables

Figures

◀

▶

◀

▶

Back

Close

Full Screen / Esc

Printer-friendly Version

Interactive Discussion



$$\rho_3 = \frac{4}{3} \sin(\alpha) - \frac{2}{3} \sin(3\alpha) + \frac{2}{15} \sin(5\alpha). \quad (13)$$

The coefficients ρ_1 , ρ_2 and ρ_3 quantify the contributions made by linear, quadratic and cubic frictional interaction, respectively. We observe that the values of ρ_1 and ρ_3 are decreased with φ and they reduce to 0 for $\varphi < 1$. For the case of $\varphi \geq 1$, $\rho_0 = \rho_1 = \rho_3 = 0$ and $\rho_2 = -\pi$, with the result that the friction term (Eq. 8) reduces to $F = U^2 / (K^2 h^{-4/3})$. If $\varphi = 0$ (or $Q = 0$), $\rho_0 = \rho_2 = 0$, $\rho_1 = 16/15$ and $\rho_3 = 32/15$, so that Eq. (8) reduces to:

$$F = \frac{16}{15\pi} \frac{v^2}{K^2 h^{-4/3}} \left[\frac{U}{v} + 2 \left(\frac{U}{v} \right)^3 \right]. \quad (14)$$

In Fig. 2, we see the contour plot displaying the main dependent parameters computed by solving the set of Eqs. (3)–(6) over a wide range of estuary shape ($0 < \gamma < 4$), and friction ($0 < \chi < 5$) for given values of $\zeta = 0.1$, $\varphi = 0.5$, $r_S = 1$.

2.3 Contributions of tide, river, tide–river interaction to the mean water level

Following Vignoli et al. (2003) and Cai et al. (2014b), the mean water level gradient with respect to distance is approximated by:

$$\frac{\partial \bar{z}}{\partial x} = -\bar{F} = -\frac{1}{K^2 h^{-4/3} \pi} (\rho_0 v^2 + \rho_2 vU + \rho_2 U^2 + \rho_3 U^3 / v), \quad (15)$$

where \bar{z} is the mean water level or residual water level (the overbar denotes the tidally averaged value). Substituting the total velocity U from Eq. (9) into the friction term F in Eq. (15) leads to three components contributing to the increase of mean water level:

a tidal component

$$\bar{F}_t = \frac{1}{K^2 h^{-4/3} \pi} \left(\frac{1}{2} \rho_2 + \rho_0 \right) v^2, \quad (16)$$

a riverine component

$$\bar{F}_r = \frac{1}{K^2 h^{-4/3} \pi} (\rho_2 - \rho_3 \varphi) U_r^2, \quad (17)$$

and tide–river interaction

$$\bar{F}_{tr} = \frac{1}{K^2 h^{-4/3} \pi} \left(-\rho_1 - \frac{3}{2} \rho_3 \right) \nu U_r. \quad (18)$$

Figure 3 shows the analytically computed gradient of the water surface over a wide range of river flow velocities ($U_r = 0\text{--}2 \text{ ms}^{-1}$) and tidal velocity amplitudes ($\nu = 0\text{--}2 \text{ ms}^{-1}$) for given $\bar{h} = 10 \text{ m}$ and $K = 45 \text{ m}^{1/3} \text{ s}^{-1}$. In general, we see that both river flow velocity and velocity amplitude trigger an increase of the water surface gradient and hence the mean tidal water level.

With the thus obtained water surface gradient $\partial \bar{z} / \partial x$, the mean water surface is given by:

$$\bar{z} = \int_0^x \frac{\partial \bar{z}}{\partial x} dx = - \int_0^x \bar{F} dx = - \int_0^x (\bar{F}_t + \bar{F}_r + \bar{F}_{tr}) dx. \quad (19)$$

An iterative procedure is involved to determine the mean water surface because the analytical expression 19 contains two unknown variables, the velocity amplitude ν and the updated water depth expressed as $\bar{h}_{\text{new}} = \bar{h} + \bar{z}$.

It was shown by Godin (1991, 1999) that the quadratic velocity $U|U|$ in the friction term can be linearized by means of adopting the first and third order terms as a function of nondimensionlized velocity scaled by the maximum possible value of the velocity (i.e., $\nu + U_r$ in our case). Similar results as in Eqs. (16)–(18) can be obtained by Godin's approximation, which are presented in Appendix.

HESSD

12, 8381–8417, 2015

Analytical approach for determining mean water level profile

H. Cai et al.

Title Page

Abstract

Introduction

Conclusions

References

Tables

Figures

◀

▶

◀

▶

Back

Close

Full Screen / Esc

Printer-friendly Version

Interactive Discussion



2.4 Solution for the entire estuary

The dependent parameters δ , μ , λ and ε represent the localized tidal dynamics since they depend on local (fixed position) values of the dimensionless tidal amplitude ζ , the shape of the estuary γ , the bottom friction χ , and the dimensionless river discharge φ .

In order to correctly reproduce the main tidal hydrodynamics along the entire estuary axis, we adopt a multi-reach approach by subdividing the entire estuary into multiple reaches to account for the longitudinal variations of the cross-sections (such as water depth and bottom friction). For given amplification number δ and tidal amplitude at a certain point, the tidal amplitude at a distance Δx (such as 1 km) inland can be determined by a simple explicit integration. In this way the entire estuary can be covered by step-wise integration.

3 Application to the Yangtze estuary

3.1 Overview of the Yangtze estuary

The Yangtze river, which is the largest and longest river in South Asia, originates from the Tibetan Plateau and debouches into the East China Sea (Fig. 4). The Yangtze estuary has a branched structure. Downstream from Xuliujing, the estuary is subdivided into the South Branch and North Branch divided by the Chongming Island (see Fig. 4). The South Branch is the main channel conveying both fresh water discharge and sediment into the East China Sea, while the North Branch is barely connected to the main channel and functions in isolation (Zhang et al., 2012). Hence in this paper, we concentrate on the tidal wave propagation along the South Branch and the upper reach.

The total length of the Yangtze estuary is around 600 km starting from the mouth, located at the Hengsha gauging station, up to the station of Datong, where the influence of tidal flow is vanishing. The estuary has a meso-scale tide with a maximum and mean

HESSD

12, 8381–8417, 2015

Analytical approach for determining mean water level profile

H. Cai et al.

Title Page

Abstract

Introduction

Conclusions

References

Tables

Figures

⏪

⏩

◀

▶

Back

Close

Full Screen / Esc

Printer-friendly Version

Interactive Discussion



tidal range of 4.62 and 2.67 m near the estuary mouth, respectively. The predominant tidal constituent in the Yangtze estuary is semi-diurnal, with averaged ebb and flood duration of 7.4 and 5 h near the estuary mouth, respectively (Zhang et al., 2012). On the basis of observed data at Datong hydrological station from 1950–2012, the annual mean fresh water discharge is $28\,200\text{ m}^3\text{ s}^{-1}$ and the monthly mean fresh water discharge reaches a maximum of $49\,500\text{ m}^3\text{ s}^{-1}$ in July and a minimum of $11\,300\text{ m}^3\text{ s}^{-1}$ in January. It has been suggested that the Canter–Cremers number (representing the ratio of the amount of fresh water to saline water entering the estuary during a tidal period) during a mean spring tide is around 0.1 during the dry season while it is about 0.24 during the wet season, which suggests a partially mixed salt intrusion in the South Branch, where a well-mixed situation occurs during the dry season especially during the spring tide, when the Canter–Cremers number is less than 0.1 (Zhang et al., 2011).

3.2 Geometry of the Yangtze estuary

The topography used in this paper was obtained based on the navigation charts in 2007 having corrected to mean sea level of Huanghai1985 datum. In Fig. 5, the geometric characteristics (i.e., the cross-sectional area, the stream width, the estuary depth) along the Yangtze estuary axis together with the best fitting curves are shown. We see that both the cross-sectional area and stream width can well represented by using functions of Eqs. (1) and (2), which converge exponentially towards a constant cross-section in the river part. The positions of the cross-sections are presented in Fig. 4 as red line segments. It is noted that the conventional approach of using ordinary exponential functions (that converge to zero) can only be used if the estuary is subdivided into two reaches, i.e., a more strongly convergent channel in the seaward part and a more prismatic channel in the landward part of the estuary, with an inflection point at the position where the geometry switches from a funnel-shaped estuary to a more prismatic channel (e.g., Cai et al., 2014a). The newly proposed Eqs. (1) and (2), however, describe the shape of the entire estuary as an entity, using only one convergence scale, the convergence lengths a and b . From Fig. 5, we observe that the

Analytical approach for determining mean water level profile

H. Cai et al.

Title Page

Abstract

Introduction

Conclusions

References

Tables

Figures



Back

Close

Full Screen / Esc

Printer-friendly Version

Interactive Discussion



($\varphi = 1$). We note that both p_1 and p_3 in Eq. (18) are equal to 0 when $\varphi > 1$, thus the tide–river component is negligible in the upstream reach of the estuary the influence of river flow is dominant over the tidal flow. Interestingly, in the transitional zone where φ is close to 1, we see that all three components are crucial for the water level slope since they are proportional to the square of the velocity scale (see Eqs. 16–18). With regard to the contribution made by tidal forcing, we observe that it increases to a maximum value near the critical position with $\varphi = 1$, beyond which it reduces until zero is reached asymptotically. On the other hand, the riverine contribution is monotonously decreasing in the seaward direction. The jump observed around $x = 245$ km has to do with the adoption of different friction coefficient in the analytical model. Meanwhile, a slightly negative contribution from tidal forcing is observed near the estuary mouth for the dry season case (see Fig. 9c), which is due to the positive value of the factor $p_2/2 + p_0$ in Eq. (16).

3.5 Prediction of high water and low water levels

Accurate prediction of the water level and its variation under external forcing (tide, river) is very important for water management to evaluate the influence of river floods, man-made structures (e.g., storm surge barriers, flood gates), and ecosystems protections. In particular, reliable estimation of high water ($\bar{h} + \eta$) and low water ($\bar{h} - \eta$) levels is necessary for flood control and in case problems arise with regard to fresh water withdrawal and navigation. In order to explore the response of high water and low water levels to the fresh water discharge, scenario simulation under given mean tidal amplitude ($\eta_0 = 1.3$ m) and spring tidal amplitude ($\eta_0 = 2.3$ m) were conducted. The results are shown in Fig. 10. In general, we see that both high water and low water levels increase in landward direction for different fresh water discharge conditions. Only during low flows, we see in Fig. 10a and b that the high water level reaches a maximum value. This is illustrated in Fig. 11.

Figure 11 presents the case of extreme high water occurring near the transitional zone of the Yangtze estuary for a spring tide amplitude $\eta_0 = 2.3$ m and a small fresh

Analytical approach for determining mean water level profile

H. Cai et al.

Title Page

Abstract

Introduction

Conclusions

References

Tables

Figures

⏪

⏩

◀

▶

Back

Close

Full Screen / Esc

Printer-friendly Version

Interactive Discussion



water discharge $Q = 10\,000\text{ m}^3\text{ s}^{-1}$. The reason for this phenomenon lies in longitudinal variation of the depth, which has its maximum value near the transition zone. The larger depth causes less friction, which favours amplification. At higher discharges, the friction term gains prominence and the amplification disappears.

It is worth examining the likelihood of extreme high water level (EHWL) as a function of the probability of exceedence along the estuary since EHWL is closely linked to flood control and planning of future engineering works (e.g., dam construction, channel deepening, confinement or widening of channels). In this paper, we used the three-parameter generalized extreme-value (GEV) distribution to interpret the probability distribution of EHWL. The method has been extensively used in a wide range of regional frequency analysis, such as annual floods, rainfall, wave height, and other natural extremes (Martins and Stedinger, 2000). For given positive random variable k , the cumulative distribution function of the GEV distribution is given by

$$F(k; \alpha_1, \alpha_2, \alpha_3) = \exp \left\{ - \left[1 + \alpha_3 \left(\frac{k - \alpha_1}{\alpha_2} \right) \right]^{-1/\alpha_3} \right\}, \quad (20)$$

where α_1 , α_2 , and α_3 represent shape, location, and scale of the distribution function, respectively. The critical value k_r , which is defined as a value that is expected to be equalled or exceeded on average once every interval of time T_r (with probability of $1/T_r$), can be computed by solving the equation of $F(k_r; \alpha_1, \alpha_2, \alpha_3) = 1 - 1/T_r$ and is given by

$$k_r = \frac{[-\ln(1 - 1/T_r)]^{-\alpha_3} \alpha_2 - \alpha_2 + \alpha_1 \alpha_3}{\alpha_3}. \quad (21)$$

In this paper, we first calculated the GEV distribution of maximum mean daily discharge at Datong gauging station based on the available historical record from 1947 to 2012 (see Fig. 12a). The three parameters were estimated by the method of maximum

HESSD

12, 8381–8417, 2015

Analytical approach for determining mean water level profile

H. Cai et al.

Title Page

Abstract

Introduction

Conclusions

References

Tables

Figures



Back

Close

Full Screen / Esc

Printer-friendly Version

Interactive Discussion



tidal river can be described by Eqs. (1) and (2), where the convergence lengths (a and b) account for the transition from the funnel estuary in the seaward part to the prismatic channel in the upstream part. The other important assumption is that the analytical solutions of water level and velocity can be described by a residual term (residual water level or river flow velocity) in combination with a simple harmonic wave, which suggests that the model does not account for the interaction between different tidal constituents (e.g., M_2 and M_4). However, since we focus on the reproduce of the first-order hydrodynamics this is not a critical limitation.

The hydrodynamics model has been used to reproduce the main dynamics in the Yangtze estuary, which shows good correspondence with observed data. The model is subsequently used to explore the longitudinal variation of mean water level under a wide range of tidal amplitude and fresh water discharge conditions. It is shown that both tidal amplitude and fresh water discharge tend to rise the mean water level along the Yangtze estuary as a result of the nonlinear frictional dissipation. Specifically, the mean water level is influenced primarily by the tide–river interaction in tide-dominated region, while it is mainly controlled by the river flow in the upstream part of the estuary. The contribution made by pure tidal influence only becomes important in the transitional zone, where the river flow velocity to tidal velocity amplitude ratio approximately equals 1. Finally, we also demonstrate that the proposed method can be used to predict the envelopes of high water and low water, which is very useful when assessing the potential influence of intensified extreme river floods and human interventions (e.g., dredging for navigational channel or fresh water withdrawal along the estuary) on along-channel water levels. More importantly, the analytical approach in combination with extreme value theory can be used to estimate the extreme high water level frequency distribution and the likelihood of various extreme values as a function of return period, which makes the proposed method a useful tool for water management (e.g., flood control measures).

HESSD

12, 8381–8417, 2015

Analytical approach for determining mean water level profile

H. Cai et al.

Title Page

Abstract

Introduction

Conclusions

References

Tables

Figures



Back

Close

Full Screen / Esc

Printer-friendly Version

Interactive Discussion



Appendix: Derivation of the contributions made by tide and river to the water level slope using Godin's approach

Godin (1991, 1999) derived an accurate approximation of the friction term that retained only the first and third order terms of the dimensionless velocity:

$$F_G = \frac{16}{15\pi} \frac{U'^2}{K^2 h^{-4/3}} \left[\frac{U}{U'} + 2 \left(\frac{U}{U'} \right)^3 \right], \quad (\text{A1})$$

where subscript G denotes Godin, and U' is maximum possible value of the velocity, defined as

$$U' = v + U_r. \quad (\text{A2})$$

Substituting the total velocity U from Eq. (9) into the friction term F_G (Eq. A1) and integrating over a tidal period yield components that contributes to the increase of mean water level:

the tidal component

$$\overline{F_{t-G}} = -\frac{16}{15\pi} \frac{1}{K^2 h^{-4/3}} \frac{\varphi}{1 + \varphi} 4v^2, \quad (\text{A3})$$

the riverine component

$$\overline{F_{r-G}} = -\frac{16}{15\pi} \frac{1}{K^2 h^{-4/3}} \frac{\varphi}{1 + \varphi} 3U_r^2, \quad (\text{A4})$$

and the tide–river interaction

$$\overline{F_{tr-G}} = -\frac{16}{15\pi} \frac{1}{K^2 h^{-4/3}} \frac{\varphi}{1 + \varphi} 2vU_r. \quad (\text{A5})$$

Acknowledgements. This research was financially supported by National Natural Science Foundation of China with the reference No. of 41476073.

Analytical approach for determining mean water level profile

H. Cai et al.

Title Page

Abstract

Introduction

Conclusions

References

Tables

Figures



Back

Close

Full Screen / Esc

Printer-friendly Version

Interactive Discussion



References

- Buschman, F. A., Hoitink, A. J. F., van der Vegt, M., and Hoekstra, P.: Subtidal water level variation controlled by river flow and tides, *Water Resour. Res.*, 45, W10420, doi:10.1029/2009WR008167, 2009. 8383, 8397
- 5 Cai, H., Savenije, H. H. G., and Jiang, C.: Analytical approach for predicting fresh water discharge in an estuary based on tidal water level observations, *Hydrol. Earth Syst. Sci.*, 18, 4153–4168, doi:10.5194/hess-18-4153-2014, 2014a. 8386, 8387, 8392
- Cai, H., Savenije, H. H. G., and Toffolon, M.: Linking the river to the estuary: influence of river discharge on tidal damping, *Hydrol. Earth Syst. Sci.*, 18, 287–304, doi:10.5194/hess-18-287-2014, 2014b. 8384, 8385, 8386, 8387, 8389
- 10 Dottori, F., Martina, M. L. V., and Todini, E.: A dynamic rating curve approach to indirect discharge measurement, *Hydrol. Earth Syst. Sci.*, 13, 847–863, doi:10.5194/hess-13-847-2009, 2009. 8382
- Dronkers, J. J.: *Tidal Computations in River and Coastal Waters*, Elsevier, New York, 1964. 8383, 8388
- 15 Gay, P. and O'Donnell, J.: Comparison of the salinity structure of the Chesapeake Bay, the Delaware Bay and Long Island sound using a linearly tapered advection-dispersion model, *Estuar. Coast.*, 32, 68–87, doi:10.1007/s12237-008-9101-4, 2009. 8385
- Gay, P. S. and O'Donnell, J.: A simple advection-dispersion model for the salt distribution in linearly tapered estuaries, *J. Geophys. Res.*, 112, C07021, doi:10.1029/2006jc003840, 2007. 8385
- 20 Godin, G.: Compact approximations to the bottom friction term, for the study of tides propagating in channels, *Cont. Shelf Res.*, 11, 579–589, doi:10.1016/0278-4343(91)90013-V, 1991. 8383, 8390, 8399
- 25 Godin, G.: The propagation of tides up rivers with special considerations on the upper Saint Lawrence river, *Estuar. Coast Shelf S.*, 48, 307–324, doi:10.1006/ecss.1998.0422, 1999. 8383, 8390, 8399
- Godin, G. and Martinez, A.: Numerical experiments to investigate the effects of quadratic friction on the propagation of tides in a channel, *Cont. Shelf Res.*, 14, 723–748, doi:10.1016/0278-4343(94)90070-1, 1994. 8383
- 30

HESSD

12, 8381–8417, 2015

Analytical approach for determining mean water level profile

H. Cai et al.

Title Page

Abstract

Introduction

Conclusions

References

Tables

Figures

⏪

⏩

◀

▶

Back

Close

Full Screen / Esc

Printer-friendly Version

Interactive Discussion



**Analytical approach
for determining mean
water level profile**

H. Cai et al.

[Title Page](#)[Abstract](#)[Introduction](#)[Conclusions](#)[References](#)[Tables](#)[Figures](#)[⏪](#)[⏩](#)[◀](#)[▶](#)[Back](#)[Close](#)[Full Screen / Esc](#)[Printer-friendly Version](#)[Interactive Discussion](#)

- Guo, L., van der Wegen, M., Jay, D. A., Matte, P., Wang, Z. B., Roelvink, D. J., and He, Q.: River-tide dynamics: exploration of non-stationary and nonlinear tidal behavior in the Yangtze River estuary, *J. Geophys. Res.*, 120, 3499–3521, doi:10.1002/2014JC010491, 2015. 8384
- Ippen, A. T.: *Tidal Dynamics In Estuaries, Part I: Estuaries of Rectangular Section*, McGraw-Hill, New York, 494–522, 1966. 8385
- Jay, D. A. and Flinchem, E. P.: Interaction of fluctuating river flow with a barotropic tide: a demonstration of wavelet tidal analysis methods, *J. Geophys. Res.*, 102, 5705–5720, doi:10.1029/96JC00496, 1997. 8383
- Jay, D. A., Leffler, K., Diefenderfer, H. L., and Borde, A. B.: Tidal-fluvial and estuarine processes in the lower Columbia River: I. Along-channel water level variations, Pacific Ocean to Bonneville Dam, *Estuar. Coast.*, 38, 415–433, doi:10.1007/s12237-014-9819-0, 2015. 8384
- Jones, B. E.: *A Method of Correcting River Discharge for a Changing Stage*, vol. Water Supply 375, U. S. Geological Survey, Washington, D.C., 117–130, 1916. 8382
- Kukulka, T. and Jay, D. A.: Impacts of Columbia River discharge on salmonid habitat: 1. A nonstationary fluvial tide model, *J. Geophys. Res.*, 108, 3293, doi:10.1029/2002JC001382, 2003a. 8383
- Kukulka, T. and Jay, D. A.: Impacts of Columbia River discharge on salmonid habitat: 2. Changes in shallow-water habitat, *J. Geophys. Res.*, 108, 3294, doi:10.1029/2003JC001829, 2003b. 8383
- LeBlond, P. H.: Forced fortnightly tides in shallow waters, *Atmos. Ocean*, 17, 253–264, doi:10.1080/07055900.1979.9649064, 1979. 8383
- Martins, E. S. and Stedinger, J. R.: Generalized maximum-likelihood generalized extreme-value quantile estimators for hydrologic data, *Water Resour. Res.*, 36, 737–744, doi:10.1029/1999wr900330, 2000. 8396
- Prandle, D. and Rahman, M.: Tidal response in estuaries, *J. Phys. Oceanogr.*, 10, 1552–1573, doi:10.1175/1520-0485(1980)010<1552:Trie>2.0.Co;2, 1980. 8385
- Sassi, M. G. and Hoitink, A. J. F.: River flow controls on tides and tide-mean water level profiles in a tidal freshwater river, *J. Geophys. Res.*, 118, 4139–4151, doi:10.1002/Jgrc.20297, 2013. 8383, 8397
- Savenije, H. H. G.: Analytical expression for tidal damping in alluvial estuaries, *J. Hydraul. Eng.*, 124, 615–618, doi:10.1061/(ASCE)0733-9429(1998)124:6(615), 1998. 8385
- Savenije, H. H. G.: A simple analytical expression to describe tidal damping or amplification, *J. Hydrol.*, 243, 205–215, doi:10.1016/S0022-1694(00)00414-5, 2001. 8385

- Savenije, H. H. G.: Salinity and Tides in Alluvial Estuaries, Elsevier, New York, 2005. 8383, 8384, 8385
- Savenije, H. H. G.: Salinity and Tides in Alluvial Estuaries, completely revised 2nd edn., available at: www.salinityandtides.com (last access: 10 June 2015), 2012. 8383, 8384, 8385
- 5 Savenije, H. H. G., Toffolon, M., Haas, J., and Veling, E. J. M.: Analytical description of tidal dynamics in convergent estuaries, *J. Geophys. Res.*, 113, C10025, doi:10.1029/2007JC004408, 2008. 8387
- Toffolon, M., Vignoli, G., and Tubino, M.: Relevant parameters and finite amplitude effects in estuarine hydrodynamics, *J. Geophys. Res.*, 111, C10014, doi:10.1029/2005JC003104, 2006. 8385
- 10 Vignoli, G., Toffolon, M., and Tubino, M.: Non-linear frictional residual effects on tide propagation, in: *Proceedings of XXX IAHR Congress*, vol. A, 24–29 August 2003, Thessaloniki, Greece, 291–298, 2003. 8389
- Zhang, E. F., Savenije, H. H. G., Wu, H., Kong, Y. Z., and Zhu, J. R.: Analytical solution for salt intrusion in the Yangtze Estuary, China, *Estuar. Coast Shelf S.*, 91, 492–501, doi:10.1016/j.ecss.2010.11.008, 2011. 8392
- 15 Zhang, E. F., Savenije, H. H. G., Chen, S. L., and Mao, X. H.: An analytical solution for tidal propagation in the Yangtze Estuary, China, *Hydrol. Earth Syst. Sci.*, 16, 3327–3339, doi:10.5194/hess-16-3327-2012, 2012. 8391, 8392

HESSD

12, 8381–8417, 2015

Analytical approach for determining mean water level profile

H. Cai et al.

[Title Page](#)[Abstract](#)[Introduction](#)[Conclusions](#)[References](#)[Tables](#)[Figures](#)[Back](#)[Close](#)[Full Screen / Esc](#)[Printer-friendly Version](#)[Interactive Discussion](#)

Analytical approach for determining mean water level profile

H. Cai et al.

Title Page

Abstract

Introduction

Conclusions

References

Tables

Figures

◀

▶

◀

▶

Back

Close

Full Screen / Esc

Printer-friendly Version

Interactive Discussion



Table 2. The geometric characteristics of the Yangtze estuary.

Characteristics	\bar{A}_r or \bar{B}_r (m)	\bar{A}_0 or \bar{B}_0 (m)	a or b (km)	R^2
Cross-sectional area \bar{A}	14 113	154 061	117	0.98
Width \bar{B}	1509	16 897	103	0.95

Analytical approach for determining mean water level profile

H. Cai et al.

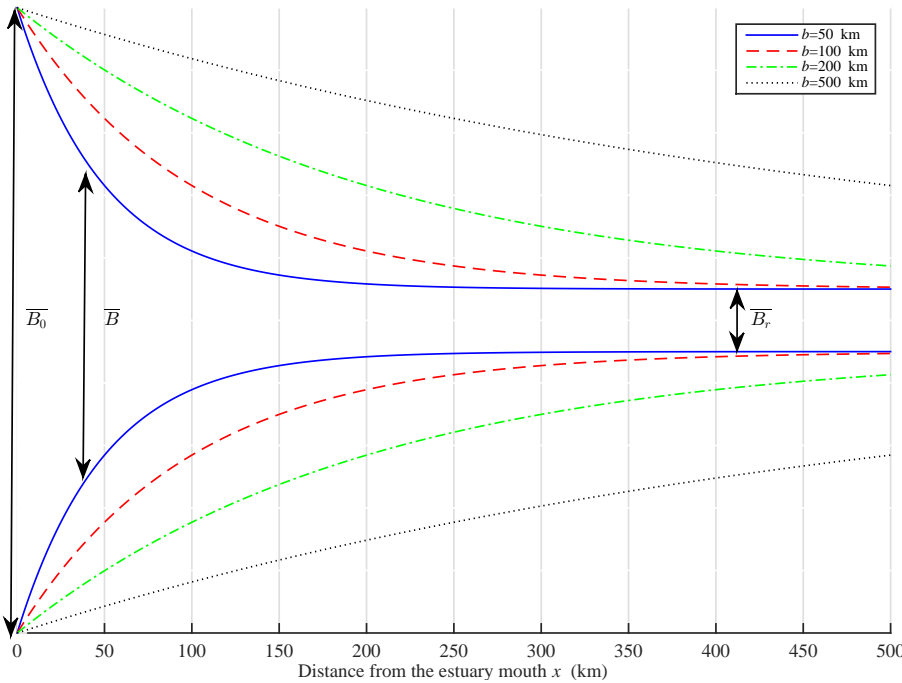


Figure 1. Variation of the estuarine shape (Eq. 2) under different width convergence length b for given values of $\bar{B}_0 = 10$ km and $\bar{B}_r = 1$ km.

Title Page

Abstract Introduction

Conclusions References

Tables Figures

◀ ▶

◀ ▶

Back Close

Full Screen / Esc

Printer-friendly Version

Interactive Discussion



Analytical approach for determining mean water level profile

H. Cai et al.

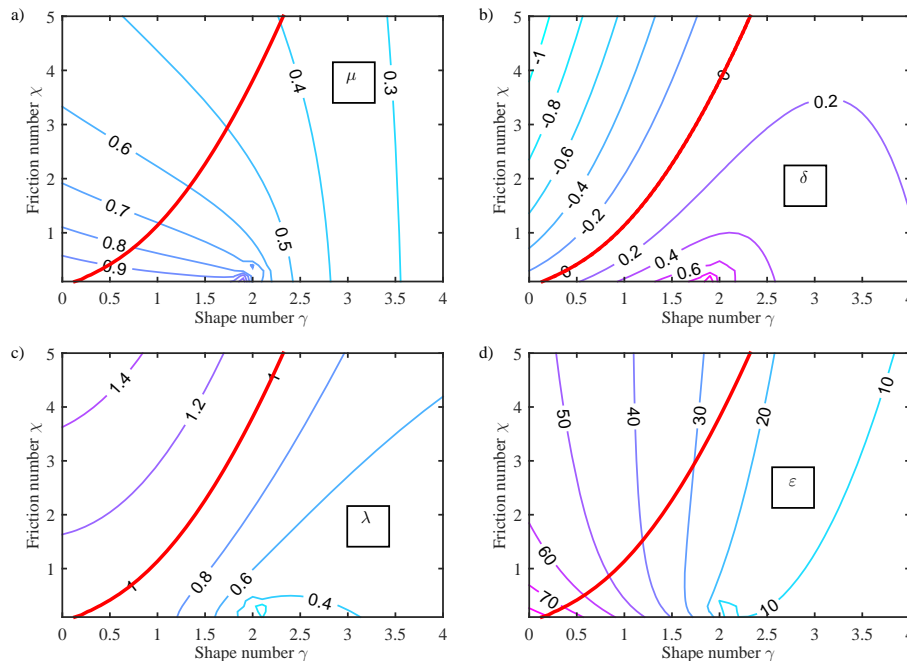


Figure 2. Analytical solutions of the four dependent dimensionless variables (**a**: velocity number μ , **b**: amplification number δ , **c**: celerity number λ , and **d**: phase lag ε) obtained by solving the set of Eqs. (3)–(6) as a function of the estuary shape number γ and the friction number χ for given values of $\zeta = 0.1$, $\varphi = 0.5$, $r_S = 1$. The thick red line represents the case for an ideal estuary ($\delta = 0$, $\lambda = 1$).

[Title Page](#)
[Abstract](#)
[Introduction](#)
[Conclusions](#)
[References](#)
[Tables](#)
[Figures](#)
[◀](#)
[▶](#)
[◀](#)
[▶](#)
[Back](#)
[Close](#)
[Full Screen / Esc](#)
[Printer-friendly Version](#)
[Interactive Discussion](#)


Analytical approach for determining mean water level profile

H. Cai et al.

Title Page

Abstract

Introduction

Conclusions

References

Tables

Figures

◀

▶

◀

▶

Back

Close

Full Screen / Esc

Printer-friendly Version

Interactive Discussion

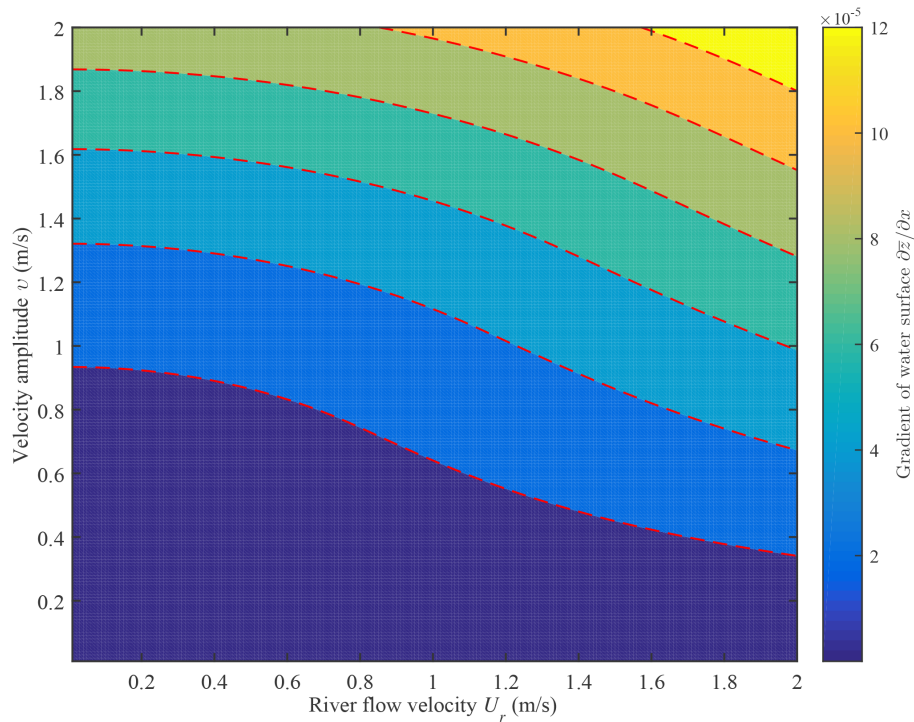


Figure 3. Contour plot of the water surface gradient $\partial \bar{z} / \partial x$ (Eq. 15) as a function of river flow velocity U_r and tidal velocity amplitude v for given tidally averaged depth $\bar{h} = 10$ m, Manning–Strickler friction coefficient $K = 45 \text{ m}^{1/3} \text{ s}^{-1}$.

Analytical approach for determining mean water level profile

H. Cai et al.

Title Page

Abstract

Introduction

Conclusions

References

Tables

Figures



Back

Close

Full Screen / Esc

Printer-friendly Version

Interactive Discussion

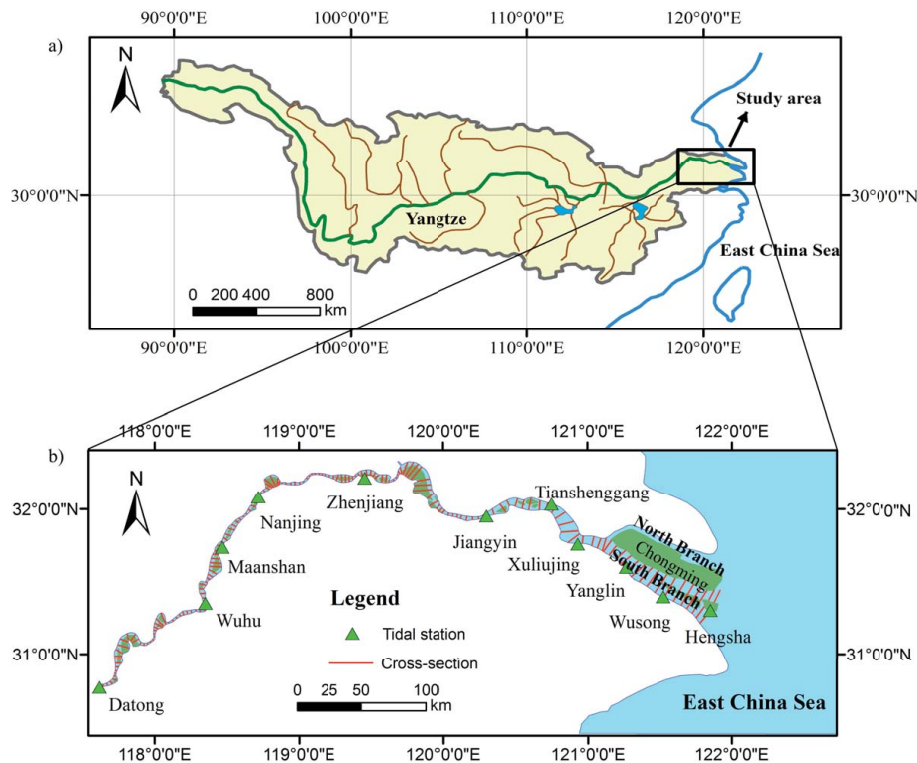


Figure 4. Location of the study area (a) and sketch of the Yangtze estuary showing the positions of the tidal stations and the cross-sections extracted along the estuary (b).

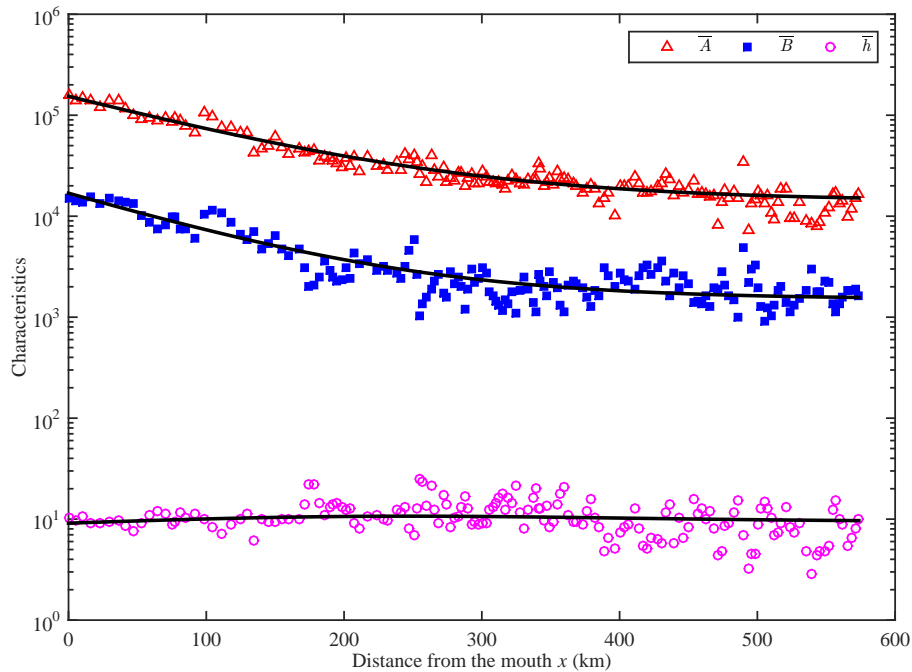


Figure 5. Semi-logarithmic plot of the geometric characteristics (the cross-sectional area \bar{A} , width \bar{B} and depth \bar{h}) along the Yangtze estuary. The drawn lines represent the best fitting curves.

**Analytical approach
for determining mean
water level profile**

H. Cai et al.

Title Page

Abstract Introduction

Conclusions References

Tables Figures

◀ ▶

◀ ▶

Back Close

Full Screen / Esc

Printer-friendly Version

Interactive Discussion



Analytical approach for determining mean water level profile

H. Cai et al.

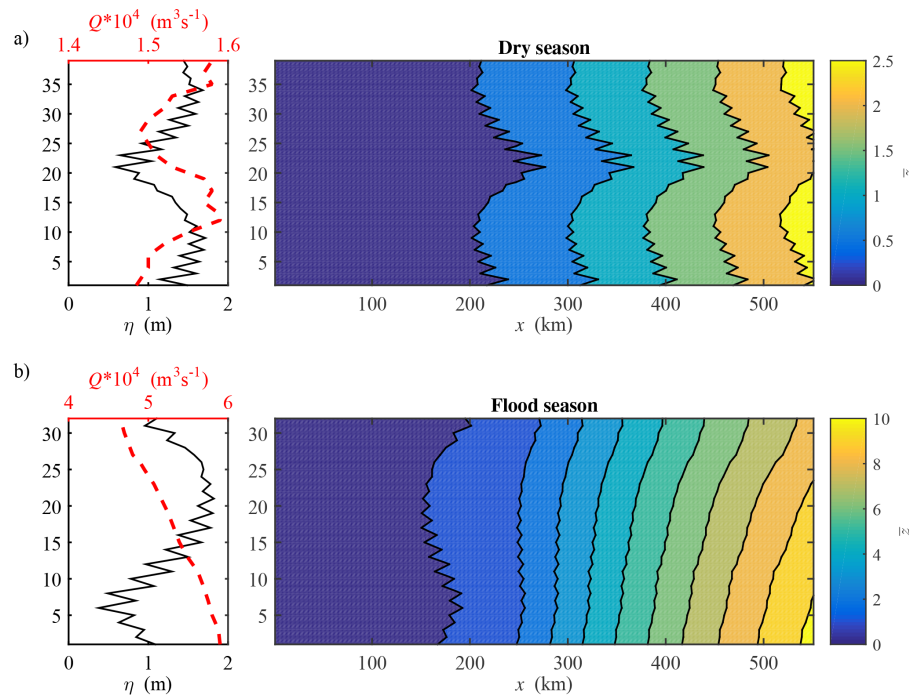


Figure 8. Longitudinal variation of the mean water level along the Yangtze estuary axis as a function of time for the dry season (a) and flood season (b). The left panel shows the corresponding observations of tidal amplitude at Hengsha station and fresh water discharge at Datong station.

Analytical approach for determining mean water level profile

H. Cai et al.

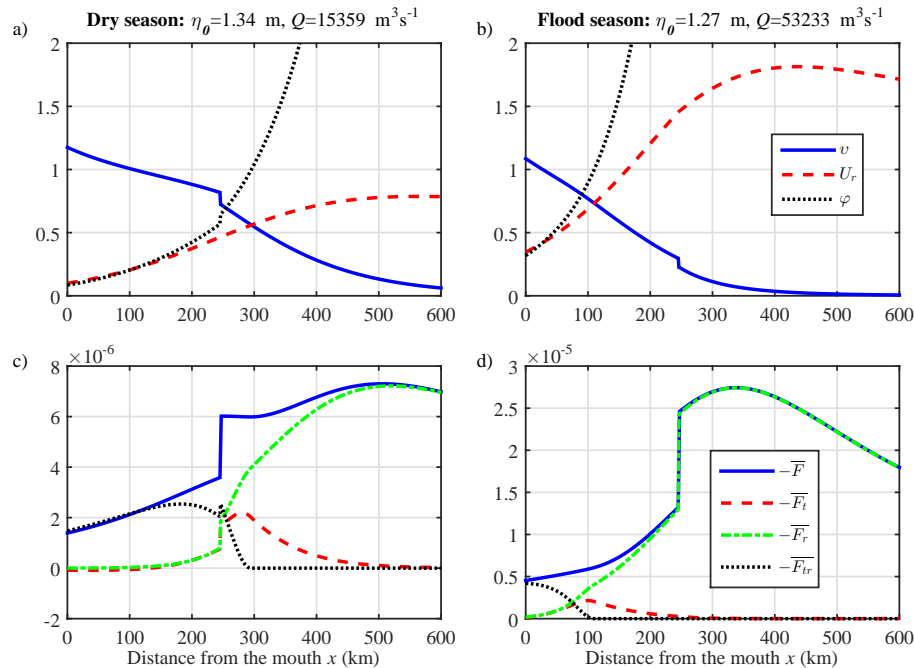


Figure 9. Longitudinal variation of the contributions to the flow velocity by river and tide (**a, b**) and contributions of river flow and tide to the water level slope (**c, d**) for the dry (**a, c**) and flood season (**b, d**) in the Yangtze estuary.

Analytical approach for determining mean water level profile

H. Cai et al.

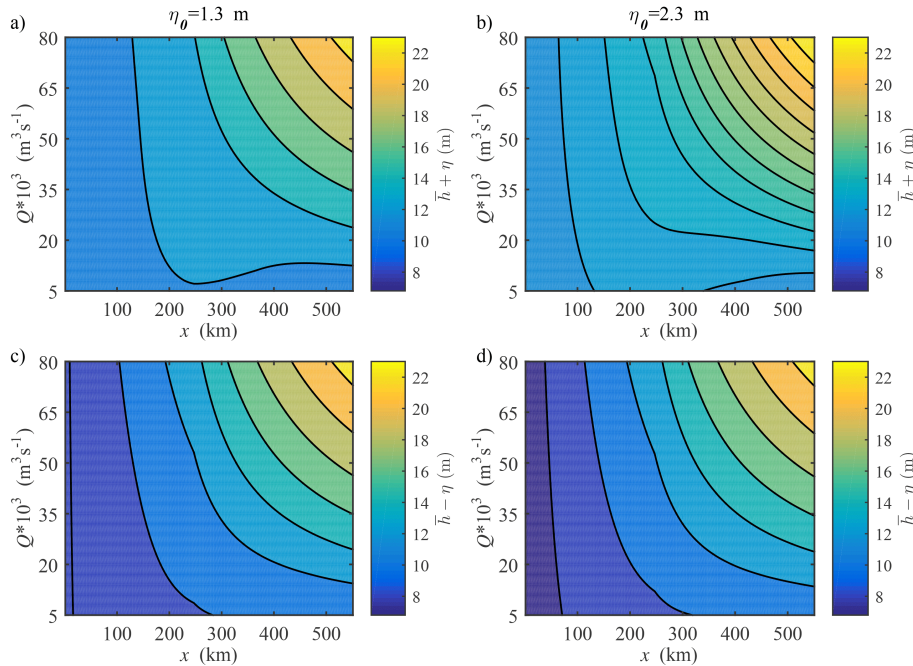


Figure 10. Longitudinal variation of the high water level $\bar{h} + \eta$ (**a, b**) and low water level $\bar{h} - \eta$ (**c, d**) as a function of fresh water discharge for given tidal amplitude at the estuary mouth (**a, c** $\eta_0 = 1.3$ m representing the mean tidal amplitude; **b, d** $\eta_0 = 2.3$ m representing the spring tidal amplitude).

[Title Page](#)
[Abstract](#)
[Introduction](#)
[Conclusions](#)
[References](#)
[Tables](#)
[Figures](#)
[◀](#)
[▶](#)
[◀](#)
[▶](#)
[Back](#)
[Close](#)
[Full Screen / Esc](#)
[Printer-friendly Version](#)
[Interactive Discussion](#)


Analytical approach for determining mean water level profile

H. Cai et al.

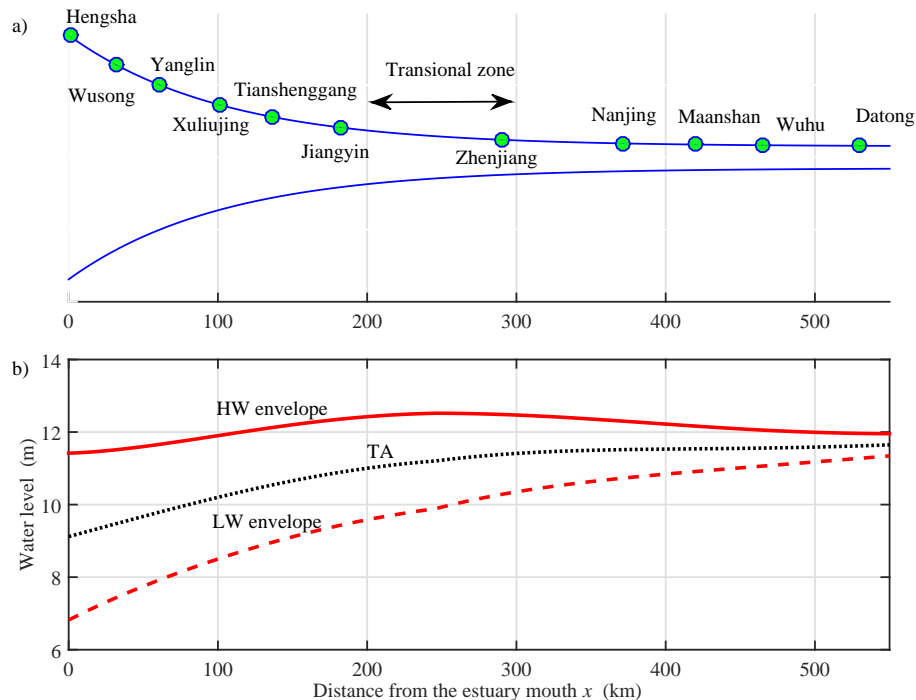


Figure 11. Shape of the Yangtze estuary **(a)** and the longitudinal computation of the high water (HW) and low water (LW) envelopes along the Yangtze estuary **(b)** for given values of $\eta_0 = 2.3$ m, $Q = 10\,000$ m³ s⁻¹. The TA curve marks tidal average values.

Analytical approach for determining mean water level profile

H. Cai et al.

Title Page

Abstract

Introduction

Conclusions

References

Tables

Figures

◀

▶

◀

▶

Back

Close

Full Screen / Esc

Printer-friendly Version

Interactive Discussion

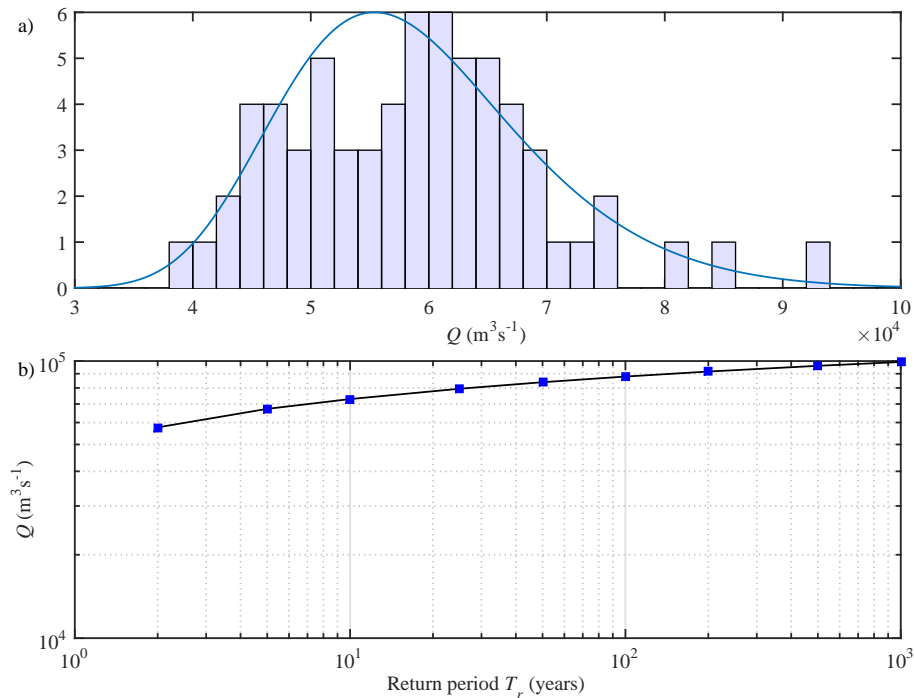


Figure 12. The fitted GEV distribution against observed maximum mean daily discharge **(a)** and the likelihood of peak discharges as a function of return period **(b)** at Datong station.